ELSEVIER

Journal of Nuclear Materials 290–293 (2001) 389–393

journal of nuclear materials

www.elsevier.nl/locate/jnucmat

Deuterium retention and lattice damage in tungsten irradiated with D ions

V.Kh. Alimov [b,*,1], K. Ertl [a], J. Roth [a]

[a] *Max-Planck-Institut für Plasmaphysik, Euratom Association, D-85748 Garching, Germany*

[b] *Institute of Physical Chemistry, Russian Academy of Sciences, Leninsky prospect 31, 117915 Moscow, Russian Federation*

Abstract

Depth profiles of D atoms and D_2 molecules in a W single crystal implanted with 6 keV D ions at 300 K have been determined using secondary ion mass spectrometry (SIMS) and residual gas analysis (RGA) measurements in the course of surface sputtering. Profiles of deuterium and lattice damage in a W single crystal irradiated with 10 keV D ions at 300 K have been investigated by means of nuclear reaction analysis (NRA) and Rutherford backscattering spectrometry combined with ion channelling techniques (RBS/C). There are at least two types of ion-induced defects which are responsible for trapping of deuterium: (i) D_2-filled microvoids (deuterium bubbles) localised in the implantation zone; and (ii) dislocations which are distributed from the surface to depths far beyond 1 μm and which capture deuterium in the form of D atoms.

Keywords: Defects; Deuterium; Deuterium depth profiling; Deuterium retention; Tungsten

1. Introduction

Tungsten has been considered for several years as a primary candidate for plasma-facing components of the divertor system in tokamaks because of its very high threshold for sputtering and high melting point [1]. Reliable data on the hydrogen behaviour in the high-Z material, in particular under irradiation, are of great importance for the application of W tiles in fusion devices.

Few data obtained by different experimental methods have been reported on hydrogen isotope retention in tungsten after implantation with H/D ions at energies in the range 0.1–8 keV [2–10]. A high percentage of the implanted hydrogen isotopes diffuses into the bulk far beyond the implantation zone even at room temperature and is captured by lattice imperfections [5,7–9].

Modelling the results of deuterium re-emission and thermal release, several authors [3,11,12] have suggested that there are two trapping sites for hydrogen isotopes implanted into W at energies below and above the threshold for displacement, respectively traps with energies in the range 0.5–0.85 eV and traps with energies at 1.2–1.4 eV. The origin of these traps is not clearly understood.

The study of microstructural evolution in tungsten during H/D ion irradiation [4,13] has shown that almost no effect is seen for hydrogen ions with energies below the threshold energy. At higher energies, dislocation loops and fine hydrogen bubbles are formed at room temperature. With increasing irradiation temperature, the fluence at which dislocation loops appear increases and the saturation density of dislocation loops decreases. At 873 K and above, only fine hydrogen bubbles are observed in a W single crystal, whereas both hydrogen bubbles and dislocation loops are formed in polycrystalline W [13]. With the use of ion-beam analysis techniques [10], the correlation between formation of dislocation loops and retention of ion-implanted deuterium has been revealed.

The purpose of this work consists of studying deuterium profiles in tungsten implanted with D ions at 300 K and obtaining detailed information on the types of

* Corresponding author. Tel.: +7-095 330 2192; fax: +7-095 334 8531.

E-mail address: alimov@ipc.rssi.ru (V.K. Alimov).

[1] Short term guest at the Max-Planck-Institut für Plasmaphysik.

0022-3115/01/$ - see front matter
PII: S0022-3115(00)00580-8

defects which are responsible for trapping of deuterium. The techniques used are secondary ion mass spectrometry combined with residual gas analysis (SIMS/RGA), nuclear reaction analysis (NRA) and Rutherford backscattering spectrometry and ion channelling (RBS/C).

2. Experimental

2.1. SIMS/RGA measurements

A W single crystal with a purity of 99.99 wt% produced by double electron-beam zone melting was used. The samples were cut from a W rod by spark cutting and were 0.6–0.7 mm in thickness. The sample surface was mechanically and electrochemically polished.

The W crystal was implanted in Moscow [14] with mass-separated 12 keV D_2^+ (6 keV D ions) at 300 K. The ion flux density was (4.5–4.7) $\times 10^{19}$ D/m^2 s. During measurements of the ion-beam current, a positive bias of 30 V was applied to the target to suppress the secondary electron emission.

Deuterium profiling for a large depth ($\geqslant 0.5$ μm) had been made possible by removal of the surface layers on the irradiated side by electrochemical polishing in 2 wt% NaOH aqueous solution. In doing so, the opposite side and edges of the sample were protected by an adhesive tape. Before and after each polishing procedure, the samples were weighed on an analytical balance and the depth of the etching was estimated from weight loss with an accuracy of ~40%. The uniformity of the electrochemical etching was controlled by optical and scanning electron microscopy.

Both after implantation and after each electropolishing procedure, the concentration of deuterium in the near-surface layers was determined by means of SIMS measurements of D^- secondary ion yields and RGA measurements of the partial pressures of HD and D_2 molecules in the course of surface sputtering. To attain a uniform erosion rate, the beam of 4 keV Ar^+ was focused to about 100 μm and was scanned over the area of 0.5×0.4 mm^2 at 45° angle to the surface. Rim effects from the sputtered crater were avoided by reducing the area of the measurement up to about 0.3×0.2 mm^2 (in the center of the sputtered spot). The use of two quadrupole mass spectrometers (QMS) made it possible to register SIMS and RGA signals simultaneously. The sputtering rate of the W single crystal was usually determined as ratio of the depth of a crater produced by sputtering on the surface (using optical interferometer) to the sputtering time with an accuracy of about 30%. After implantation, deuterium profiles were measured within a depth range 0–500 nm, whereas after each electropolishing procedure, SIMS/RGA signals were monitored during sputtering of a near-surface layer of about 15 nm thickness.

We attribute the appearance of the SIMS D^- signal to the existence of separate D atoms within the matrix [14]. A cause of the RGA D_2 signal appearance seems to be the recombination of D atoms as well as the direct release of D_2 molecules from the sputtered layers. A procedure for the separation of the recombination and molecular fractions has been described in [14]. The scale factor of D_2 concentration to RGA mass 4 intensity was estimated taking into account the sensitivity of the RGA QMS and the known sputtering rate and pumping speed. The total error of the RGA QMS calibration was about 40%.

The calibration of the D^- SIMS signal was carried out with the use of a W single crystal implanted with 20 keV D_2^+ at 100 K to fluences Φ below 3×10^{20} D/m^2 by comparing the integral SIMS signal (all over the implantation depth) with the total amount of deuterium in this sample. With this provision, the error of the calibration was estimated to be about 20%.

2.2. Ion-beam analysis

For these investigations a W single crystal was used, 1.5 mm thick with a purity of 99.995 wt% produced by double electron-beam melting. The sample surface parallel to the ⟨1 1 1⟩ plane was mechanically and electrochemically polished.

The experiments were performed in the UHV target chamber PHARAO (Garching) which was used for both ion implantation and ion-beam analysis [15]. The target chamber is connected to a 100 keV implanter and a 2.5 MeV van de Graaff accelerator providing different ion-beam analysis techniques.

The sample was mounted on a two-axis goniometer and surrounded by a negative biased shield in order to suppress secondary electron emission. Before the D ion implantation, the W single crystal was routinely aligned to find a ⟨1 1 1⟩ axial channel using backscattering spectra for 1 MeV ^{3}He ions. The procedure was good enough to reduce the backscattering intensity to 1.5% in the channelling spectra along the ⟨1 1 1⟩ axis.

The deuterium implantation of the W crystal was performed along the ⟨1 1 1 ⟩ axis direction at 300 K with 30 keV D_3^+ (10 keV D ions) at flux densities of (3.2–3.7) $\times 10^{18}$ D/m^2 s. For the measurement of the deuterium depth profile, the target was bombarded with 1.0 MeV ^{3}He ions. The α particles (primary energy 3.5 MeV) and protons from the D(^{3}He, α) H nuclear reaction were energy analysed by a small solid angle surface barrier detector positioned at 75° to the sample normal resulting in a 105° scattering angle. The particles spectrum was transformed into a depth profile of deuterium concentration with the computer program LORI [16] using nuclear cross-section data measured by Möller and Besenbacher [17], and electronic stopping power data

compiled by Ziegler [18]. For D in W, a depth resolution of about 10 nm could be achieved.

To study the lattice disorder produced by the D ion implantation, the channelling experiments along ⟨1 1 1⟩ axial direction were performed using the backscattering of ^{3}He ions with the incident energy of 0.69–1.8 MeV. The backscattered ^{3}He ions were energy analysed at a scattering angle of 165° by a second small angle surface barrier detector. For detection of the random spectra, the sample was rotated around an axis 6° off the ⟨1 1 1⟩ channelling direction. For the analysis of channelling spectra, electronic stopping power data for random incidence [18] were used.

3. Results

3.1. Deuterium depth profiles

SIMS/RGA depth profiles of D atoms and D_2 molecules in the W single crystal irradiated at 300 K with 6 keV D ions are shown in Fig. 1. The profiles of D atoms and D_2 molecules do not concur with the ion projected ranges. With an increase of the fluence Φ, the D atom concentration C_D in the implantation zone (i.e. within the near-surface layer of about 150 nm in thickness) reaches the value of about 1.2×10^{27} atoms/m^3 (~0.02 D/W) and practically does not change thereafter (Fig. 1(a)). Even at a lower fluence of 3.2×10^{20} D/m^2, the D atom profile shows a long tail extending to 300 nm, i.e. beyond the ion-implantation zone. As the fluence increases, the depth of D atom capture is enlarged and reaches ~2 μm at $\Phi \approx 1 \times 10^{23}$ D/m^2 (insert in Fig. 1 (a)).

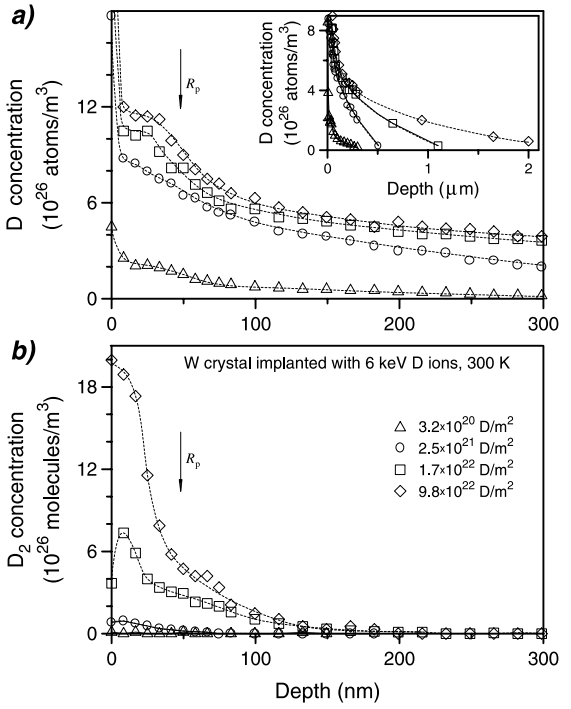

Fig. 1. Depth profiles of deuterium trapped as D atoms (a) and in the form of D_2 molecules (b) in W single crystal and hot-rolled W implanted with 6 keV D ions at 300 K as determined by combined SIMS/RGA method. The arrow indicates the mean projected range of D ions calculated by the TRIM.SP program [19]. The insert shows depth distributions of D atoms in the bulk of the samples.

The analysis of D_2 depth profiles shows that: (i) the formation of deuterium molecules in the W crystal starts at $\Phi \geqslant 2 \times 10^{21}$ D/m^2 (Fig. 1(b)), i.e. at $C_D \geqslant 1.5$ at.% (Fig. 1(a)); and (ii) D_2 molecules are localised in the ion-implantation zone alone. While C_D at a depth of about 15 nm increases by about 50% when raising Φ from 2.5×10^{21} to 9.8×10^{22} D/m^2 (Fig. 1(a)), the concentration of D_2 molecules, C_{D_2}, increases by more than an order of magnitude, reaching a value of $\sim 2 \times 10^{27}$ molecules/m^3 (~0.03 D_2/W) (Fig. 1(b)).

SIMS/RGA depth profiles of all D trapped in the W crystal, both in the form of D atoms and D_2 molecules, and NRA depth profiles (Fig. 2) are characterised by a maximum at a depth of (0.4–0.5)R_p (where R_p is the ion mean projected range) and a gradual decrease with increasing depth. The maximum D concentration in the implantation zone is found to be about 0.1 D/W. At $\Phi \geqslant 1 \times 10^{22}$ D/m^2, a long tail of D profile with a concentration of about 0.01 D/W extending far beyond the implantation zone is observed. The feature of the NRA profile, especially at a high fluence, is the significant broadening of D maximum up to a depth of ~3 R_p. It is good to bear in mind that 10 keV D ions were implanted along the ⟨1 1 1⟩ axial direction and the distribution of deuterium traps is thought to be different from those for the case of random implantation with 6 keV D ions.

3.2. Lattice damage depth profiles

When a single crystal is bombarded with an MeV beam of ^{3}He particles directed along a close-packed row of host atoms, the ions will penetrate into the crystal channels along the row (channelled fraction); part of the ions will be scattered at surface atoms and follow a 'random' trajectory (dechannelled fraction). Interaction of the channelled particles with defects causes an increase of the dechannelled fraction. The dechannelled fraction is characterized by the ratio $\chi(x)$ of the backscattering yield for incidence along a close-packed row to the yield for random incidence. The depth x is determined by converting the energy scale to a depth scale, using random stopping power for both the incoming and outgoing particles. The yield of an ion-implanted (damaged) spot χ_d is compared with the yield of an unimplanted (virgin) spot χ_v of the same crystal. The

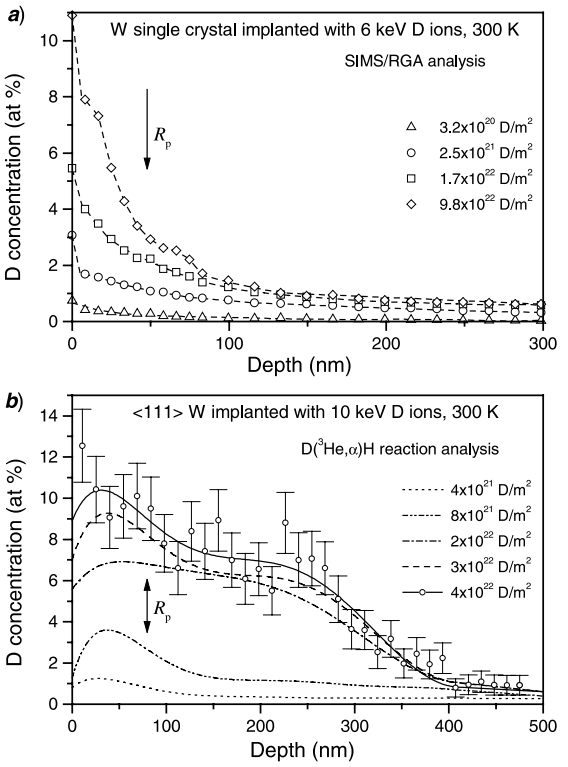

Fig. 2. Depth profiles of deuterium in W single crystal implanted at 300 K with 6 keV D ions (a) and with 10 keV D ions along the $\langle 1\,1\,1\rangle$ axial direction (b). The arrows indicate the mean projected ranges of D ions calculated by the TRIM.SP program [19]. The depth distributions of D were measured with SIMS/RGA (a) and NRA (b) methods. For the case of 10 keV D ion implantation (b), the lines are polinomially smoothed fits to the data points (shown only for $\Phi = 4 \times 10^{22}$ D/m^2).

integrated dechannelling probability due to defects formed during ion implantation is given by [20,21]

$$\int_0^x \sum_i N_i(x')\sigma_i \,\mathrm{d}x' = -\ln\left(\frac{1-\chi_\mathrm{d}(x)}{1-\chi_\mathrm{v}(x)}\right), \tag{1}$$

where N_i is the defect density and σ_i is the defect dechannelling factor for each type of defect. The dechannelling probability per unit depth $\sum_i N_i(x)\sigma_i$ is obtained by differentiation. The variation of the dechannelling factor σ with the energy E of the analysing beam provides information about the nature of the defects [20–25].

As shown in our work [26], the integrated dechannelling probability for W crystal implanted at 300 K with 10 keV D ions along $\langle 1\,1\,1\rangle$ axial direction increases with the analysing beam energy and can be expressed by the sum of an energy dependent and a constant part following the equation

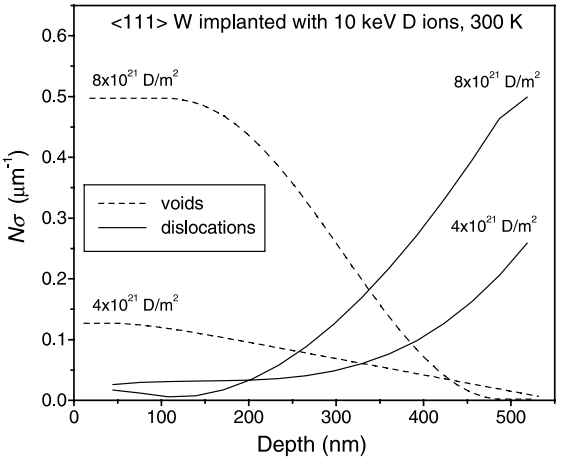

Fig. 3. The probabilities of dechannelling per unit depth as a function of depth ('depth profiles') for voids and dislocations in W crystal implanted with 10 keV D ions at 300 K to $\Phi = 4 \times 10^{21}$ and 8×10^{22} D/m^2. The values $N\sigma$ for each type of defects are determined from RBS/C spectra for 1.0 MeV ^{3}He channelling along $\langle 1\,1\,1\rangle$ axis of a W single crystal.

$$\int_0^x \sum_i N_i(x')\sigma_i(E)\,\mathrm{d}x' = K_1(x) + K_2(x)E^{1/2}, \tag{2}$$

where the coefficients K_1 and K_2 depend on the D ion fluence.

Therefore, it is reasonable to suggest that the W crystal irradiated with D ions contains at least two types of defects which are responsible for dechannelling of MeV ^{3}He ions. Based on the fact that the W crystal irradiated with D ions at 300 K contains D_2 molecules in the ion-stopping zone and taking into account the energy dependence of the dechannelling factors of various types of defects, [20–25], we conclude that the defects with E-independent dechannelling factor are D_2-filled voids (deuterium bubbles). As for the second type of defects with $E^{1/2}$-dependent dechannelling factor, only dislocations are defects of this type [22,24].

A rough idea of depth distributions of the products $N\sigma$ for microvoids and dislocations is given by differentiating the spline fitted functions $K_1(x)$ and $K_2(x)$ (for details see [26]). Microvoids are localised within the near-surface layer of ~400 nm in thickness. In turn, the dislocation density is minimal near the surface and increases with depth within the surface layer investigated (~600 nm in thickness) (Fig. 3).

4. Discussion and conclusions

The SIMS/RGA measurements have shown that irradiation of W single crystals with 6 keV D ions at 300 K leads to the accumulation of D atoms both in the ion-stopping zone (i.e. within the near-surface layer of

about 150 nm in thickness) and at depths up to several μm. In the stopping zone deuterium is additionally accumulated in the form of D_2 molecules. The maximum total concentration of retained deuterium reaches a value of ~0.10 D/W in this region.

The study of the damage structure produced in W crystals under D ion implantation and measurements of D atom and D_2 molecule profiles have revealed that there are at least two types of ion-induced defects which can be responsible for trapping of deuterium which is implanted at keV energies above the threshold for displacement: (i) D_2-filled microvoids localised in the implantation zone; and (ii) dislocations which are distributed from the surface to depths far beyond 1 μm and capture D atoms. Moreover, intrinsic (natural) defects like grain and block boundaries are thought to be responsible for the accumulation of D atoms.

According to the SIMS/RGA measurements, the formation of D_2 molecules in the implantation zone at 300 K starts at a fluence when the D atom concentration reaches ~1.5 at.%. One would conclude that this value is a minimum D atom concentration necessary for bubble formation in tungsten. Additionally, in the ion-stopping zone D atoms can be trapped by vacancies with binding energy of about 1.1 eV [27]. Another possible source of D atoms in the implantation zone is deuterium adsorbed on bubble walls [28].

The high compressive stresses created in the near-surface layers due to the formation and growth of deuterium bubbles are the reason for generation of dislocations far beyond the ion-implantation zone. Most of the D atoms implanted into tungsten at room temperature diffuse deep into the bulk and are captured by the dislocations and grain boundaries.

Acknowledgements

The authors would like to thank Dr W. Eckstein for performing TRIM.SP calculations. One of us, V. Alimov, gratefully acknowledges financial support by the Max-Planck-Institut für Plasmaphysik. The portion of this work performed at Institute of Physical Chemistry, Moscow, was supported by the US Department of Energy under Contract No. LG-9196 with Sandia National Laboratories.

References

[1] G. Federici et al., J. Nucl. Mater. 266–269 (1999) 14.
[2] A.A. Pisarev, A.V. Varava, S.K. Zhdanov, J. Nucl. Mater. 220–222 (1995) 926.
[3] C. García-Rosales, P. Franzen, H. Plank, J. Roth, E. Gauthier, J. Nucl. Mater. 233–237 (1996) 803.
[4] R. Sakamoto, T. Mugora, N. Yoshida, J. Nucl. Mater. 233–237 (1996) 776.
[5] V.Kh. Alimov, B.M.U. Scherzer, J. Nucl. Mater. 240 (1996) 75.
[6] A.A. Haasz, J.W. Davis, J. Nucl. Mater. 241–243 (1997) 1076.
[7] A.A. Haasz, J.W. Davis, M. Poon, R.G. Macaulay-Newcombe, J. Nucl. Mater. 258–263 (1998) 889.
[8] A.A. Haasz, M. Poon, J.W. Davis, J. Nucl. Mater. 266–269 (1999) 520.
[9] R. Causey, K. Wilson, T. Venhaus, W.R. Wampler, J. Nucl. Mater. 266–269 (1999) 467.
[10] S. Nagata, K. Takahiro, S. Horiike, S. Yamaguchi, J. Nucl. Mater. 266–269 (1999) 1151.
[11] P. Franzen, C. García-Rosales, H. Plank, V.Kh. Alimov, J. Nucl. Mater. 241–243 (1997) 1082.
[12] D.A. Thompson, R.G. Macaulay-Newcombe, McMaster University/CFFTR Annual Report for ITER Task T227 (1997).
[13] R. Sakamoto, T. Muroga, N. Yoshida, J. Nucl. Mater. 220–222 (1995) 819.
[14] V.Kh. Alimov, V.N. Chernikov, A.P. Zakharov, J. Nucl. Mater. 241–243 (1997) 1047.
[15] R. Siegele, J. Roth, B.M.U. Scherzer, S.J. Pennycook, J. Appl. Phys. 73 (1993) 2225.
[16] B.M.U. Scherzer, H.L. Bay, R. Behrisch, P. Børgesen, J. Roth, Nucl. Instrum. and Meth. 157 (1978) 75.
[17] W. Möller, F. Besenbacher, Nucl. Instrum. Meth. 168 (1980) 111.
[18] J.F. Ziegler, Helium stopping power and ranges in all elemental matter, in: The Stopping and Ranges of Ions in Matter, vol. 4, Pergamon, New York, 1977.
[19] W. Eckstein, Computer simulation of ion–solid interaction, in: Springer Series in Materials Science, vol. 10, Springer, Berlin, 1991.
[20] J.R. Tesmer, M. Nastasi, J.C. Barbour, C.J. Maggiore, J.W. Mayer, Handbook of Modern Ion Beam Materials Analysis, Materials Research Society, Pittsburgh, PA, 1995.
[21] L.C. Feldman, J.W. Mayer, S.T. Picraux, Material Analysis by Ion Channeling, Academic Press, New York, 1982.
[22] Y. Quéré, Phys. Stat. Sol. 30 (1968) 713.
[23] H. Kudo, Phys. Rev. B 18 (1978) 5995.
[24] J. Mory, Y. Quéré, Radiat. Eff. 13 (1972) 57.
[25] D. Ronikier-Polonsky, G. Désarmot, N. Housseau, Y. Quéré, Radiat. Eff. 27 (1975) 81.
[26] V.Kh. Alimov, K. Ertl, J. Roth, K. Schmid, Deuterium retention and lattice damage in tungsten irradiated with D ions, Phys. Scr., in press.
[27] J.R. Fransens, M.S. Abd El Keriem, F. Pleiter, J. Phys.: Condens. Matter 3 (1991) 9871.
[28] H. Eleveld, PhD Thesis, Technische Universiteit Delft, 1996.